

Using pre-COVID Postprandial Plasma Glucose Data as the Baseline to Predict Postprandial Plasma Glucose Values in the COVID Period Applying the Higher Order Equations of Interpolation Perturbation Theory from Quantum Mechanics with two Perturbation Factors of Carbs/Sugar Intake Amount and Post-Meal Walking Steps Based on GH-Method: Math-Physical Medicine (No. 464)

Gerald C Hsu

EclaireMD Foundation, USA

***Corresponding author**

Gerald C Hsu, EclaireMD Foundation, USA

Submitted: 16 July 2021; **Accepted:** 23 July 2021; **Published:** 06 Aug 2021

Citation: Gerald C Hsu (2021) Using pre-COVID Postprandial Plasma Glucose Data as the Baseline to Predict Postprandial Plasma Glucose Values in the COVID Period Applying the Higher Order Equations of Interpolation Perturbation Theory from Quantum Mechanics with two Perturbation Factors of Carbs/Sugar Intake Amount and Post-Meal Walking Steps Based on GH-Method: Math-Physical Medicine (No. 464). *J App Mat Sci & Engg Res*, 5(2), 1-7.

Abstract

The author has applied the high-order interpolation perturbation theory from quantum mechanics to his medical research work and has written numerous articles on this topic. The high-order perturbation theory application includes the first-order, second-order, and third-order of a “perturbation factor” to generate three results with different prediction accuracies. Usually the higher order perturbation factor yields a higher prediction accuracy. In general, he identifies this type of problem using one “perturbation factor” only, such as carbs/sugar for postprandial plasma glucose (PPG) or body weight for fasting plasma glucose (FPG). In this article, he attempts two “perturbation factors” simultaneously to predict his future PPG based on carbs/sugar intake amount (carbs) and post-meal walking steps (walk), while using a previously collected PPG dataset as his baseline of calculation that is “initial condition”.

At first, he accumulated a set of measured PPG data and synthesized waveform generated during the period from 5/5/2018 to 1/18/2020 known as the “pre-COVID” period. He utilized the pre-COVID synthesized dataset and high-order perturbation equation with the above-mentioned two perturbation factors to generate another synthesized PPG waveform during the on-going period from 1/19/2020 to 6/7/2021 or another future ending date (the “COVID” period). Finally, he compared this predicted PPG dataset and waveform against his measured COVID PPG data and waveform (with data collected to date) to obtain its prediction accuracy and waveform shape similarity. It should be noted that if he changes the end date for the present measurement period, he must re-examine or even modify his initially defined perturbation factors as well.

These comparison studies contain the following two final yardsticks to provide confirmation. The first yardstick is to verify the prediction accuracies of these three perturbed PPG values via their average PPG of two datasets or waveforms. The second yardstick is to examine the waveform shape similarity via their calculated correlation coefficients between the measured PPG dataset or

waveform and the three perturbed PPG datasets or waveforms.

The purpose of this study is to investigate the prediction accuracy and waveform shape similarities of PPG in his present period or future period. He utilizes three different orders of perturbation equations with two selected vital influential factors as the “perturbation factors”, which are carbs and walk, and based on a previous period’s PPG data or waveform as his prediction’s baseline of calculation.

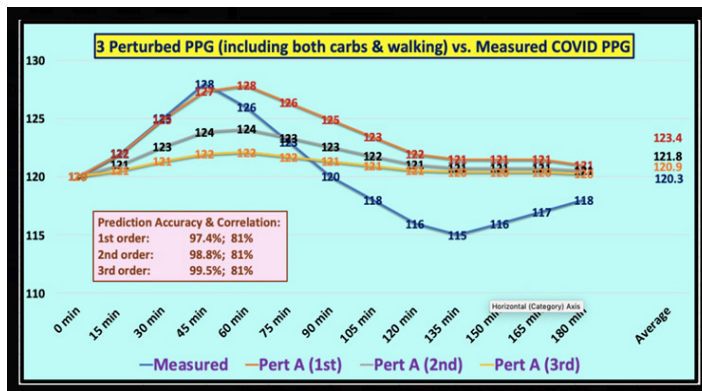
In summary, the obvious conclusion drawn from this research work is that **the perturbation equation with two perturbation factors provide a predicted PPG with a slightly higher accuracy and near-duplicative waveform shapes in comparison with one perturbation factor. As a matter of fact, the higher-order of the perturbation equation used, the better results can be achieved for prediction accuracy.**

The following table shows the prediction accuracies in the format of (carbs only and carbs combined with walk):

First order: 97.3%, 97.4%
Second order: 98.7%, 98.8%
Third order: 99.4%, 99.5%

In this study, the three perturbed PPG waveforms have equal level of waveform shape similarity with 81% versus the measured COVID PPG waveform. The correlations of lower than 90% are due to the selection on the pre-COVID PPG data as his baseline of calculation.

In the real world, there are very few diabetes doctors and patients who can understand the perturbation theory of quantum mechanics, let alone be able to apply this theory on calculation of predicted future glucose based on previous data, also including two perturbation factors, with a desired high prediction accuracy.



Introduction

The author has applied the high-order interpolation perturbation theory from quantum mechanics to his medical research work and has written numerous articles on this topic. The high-order perturbation theory application includes the first-order, second-order, and third-order of a “perturbation factor” to generate three results with different prediction accuracies. *Usually the higher order perturbation factor yields a higher prediction accuracy.* In general, he identifies this type of problem using one “perturbation factor” only, such as carbs/sugar for postprandial plasma glucose (PPG) or body weight for fasting plasma glucose (FPG). In this article, he attempts two “perturbation factors” simultaneously to predict his future PPG based on carbs/sugar intake amount (carbs) and post-meal waking steps (walk), while using a previously collected PPG dataset as his baseline of calculation that is “initial condition”.

At first, he accumulated a set of measured PPG data and synthesized waveform generated during the period from 5/5/2018 to 1/18/2020 known as the “pre-COVID” period. He utilized the pre-COVID synthesized dataset and high-order perturbation equation with the above-mentioned two perturbation factors to generate another synthesized PPG waveform during the on-going period from 1/19/2020 to 6/7/2021 or another future ending date (the “COVID” period). Finally, he compared this predicted PPG dataset and waveform against his measured COVID PPG data and waveform (with data collected to date) to obtain its prediction accuracy and waveform shape similarity. It should be noted that if he changes the end date for the present measurement period, he must re-examine or even modify his initially defined perturbation factors as well.

These comparison studies contain the following two final yardsticks to provide confirmation. The first yardstick is to verify the prediction accuracies of these three perturbed PPG values via their average PPG of two datasets or waveforms. The second yardstick is to examine the waveform shape similarity via their calculated correlation coefficients between the measured PPG dataset or waveform and the three perturbed PPG datasets or waveforms.

The purpose of this study is to investigate the prediction accuracy and waveform shape similarities of PPG in his present period or future period. He utilizes three different orders of perturbation equations with two selected vital influential factors as the “perturbation factors”, which are carbs and walk, and based on a previous period’s PPG data or waveform as his prediction’s baseline of calculation.

Methods

The author has chosen not to repeat all of the details regarding his applied methods as described in other papers. Instead, he outlines a few important equations, formulas, or conditions in this article.

MPM Background

To learn more about his developed GH-Method: math-physical medicine (MPM) methodology, readers can read the following three papers selected from the published 400+ medical papers.

The first paper, No. 386 (Reference 1) describes his MPM methodology in a general conceptual format. The second paper, No. 387 (Reference 2) outlines the history of his personalized diabetes research, various application tools, and the differences between biochemical medicine (BCM) approach versus the MPM approach. The third paper, No. 397 (Reference 3) depicts a general flow diagram containing ~10 key MPM research methods and different tools.

Higher-order Interpolation Perturbation Theory with two Perturbation Factors

The author applies the higher-order interpolation perturbation method to obtain his three “perturbed PPG” waveforms based on one function of the selected carbs/sugar intake amount functioning as *the perturbation factors*, which is the “Slope Equation”. He uses the “measured PPG” waveform as his “reference waveform”.

The following polynomial function is used as the perturbation equation:

$$A = f(x) = A_0 + (A_1 * x) + (A_2 * x^{**2}) + (A_3 * x^{**3}) + \dots + (A_n * x^{**n})$$

Where *A* is the perturbed glucose, *A_i* is the measured glucose, and *x* is the “perturbation factor” based on different carbs/sugar intake amounts.

For this particular study, he choose his **A_i** where **i=1 to 3**. Therefore, the perturbation theory equation from above can be simplified to the following form:

$$A = f(x) = A_0 + (A_1 * x) + (A_2 * (x^{**2})) + (A_3 * (x^{**3}))$$

Or the third-order interpolation perturbation equation can then be expressed in the following general format:

$$A_i = A_1 + (A_2 - A_1) * (\text{slope } 1) + (A_2 - A_1) * (\text{slope } 2) + (A_2 - A_1) * (\text{slope} * 3)$$

More specifically, the following formats of three perturbation equations are utilized in the calculations of this study:

A of first order
 $= (A_2 - A_1) * (\text{slope } 1)$

A of second order
 $= (A_2 - A_1) * (\text{slope } 2)$

A of third order
 $= (A_2 - A_1) * (\text{slope } 3)$

Where:

A_1 = original glucose A at time 1

A_2 = advanced glucose A at time 2

$(A_2 - A_1)$ = (Glucose A at Time 2 - Glucose A at Time 1)

The perturbation factor of **Slope** is an arbitrarily selected parameter that controls the size of the perturbation.

The author has chosen a function of carbs/sugar intake amount, as his perturbation factor or slope, which is further defined as follows:

In this particular study, he selects the 4.9 grams as the low-bound carbs/sugar and 21.8 grams as the high-bound carbs/sugar, while 13.2 grams as his selected carbs/sugar amount.

The equations for 3 slopes are:

Slope 1
 $= (\text{Selected Carbs} - \text{Low-bound Carbs}) / (\text{High-bound Carbs} - \text{Low-bound Carbs})$

Slope 2
 $= (\text{Slope } 1 * \text{Slope } 1)$
 or $(\text{Slope} ** 2)$

Slope 3
 $= (\text{Slope } 1 * \text{Slope } 1 * \text{Slope } 1)$
 or $(\text{Slope} ** 3)$

It should be noted that, for achieving a better predicted glucose value, the selected carbs amount should be within the range of the high-bound carbs and the low-bound carbs, where these two boundary carbs amounts should be within 4x in magnitude to each other.

Therefore, in this particular study, his three slope values are calculated as follows:

Slope 1 from Carbs = 0.53

Slope 2 from Carbs = 0.28

Slope 3 from Carbs = 0.15

In order to deal with the second perturbation factor, post-meal walking steps, he repeats the second equation similar to the above-mentioned first perturbation equation.

$$B = f(y) = B_0 + (B_1 * y) + (B_2 * (y ** 2)) + (B_3 * (y ** 3))$$

Or the third-order interpolation perturbation equation can then be expressed in the following general format:

$$B_i = B_1 + (B_2 - B_1) * (\text{slope } 1) + (B_2 - B_1) * (\text{slope } 2) + (B_2 - B_1) * (\text{slope} * 3)$$

More specifically, the following formats of the three perturbation equations are utilized in the calculations for this study:

B of first order
 $= (B_2 - B_1) * (\text{slope } 1)$

B of second order
 $= (B_2 - B_1) * (\text{slope } 2)$

B of third order
 $= (B_2 - B_1) * (\text{slope } 3)$

Where:

B_1 = original glucose B at time 1

B_2 = advanced glucose B at time 2

$(B_2 - B_1)$ = (Glucose B at Time 2 - Glucose B at Time 1)

The perturbation factor of **Slope** is an arbitrarily selected parameter that controls the size of the perturbation. The author has chosen a function of carbs/sugar intake amount, as his perturbation factor or slope, which is further defined as follows:

In this study, he selects the 3,076 steps as the low-bound walking and 5,529 steps as the high-bound walking, while 4,356 steps as his selected post-meal walking amount.

The equations for the 3 slopes are:

Slope 1
 $= (\text{Selected Walk} - \text{Low-bound Walk}) / (\text{High-bound Walk} - \text{Low-bound Walk})$

Slope 2
 $= (\text{Slope } 1 * \text{Slope } 1)$
 or $(\text{Slope} ** 2)$

Slope 3
 $= (\text{Slope } 1 * \text{Slope } 1 * \text{Slope } 1)$
 or $(\text{Slope} ** 3)$

Therefore, in this particular study, his three slope values are calculated as follows:

Slope 1 from Walk = 0.52
Slope 2 from Walk = 0.27
Slope 3 from Walk = 0.14

It should be pointed out that *these three slopes from walk are 0.01 less than the three slopes from carbs due to the prediction accuracy from one perturbation factor of carbs only is 0.1% lower than the prediction accuracy from two perturbation factors of carbs combined with walk.*

Slope 1 from Carbs = 0.53
Slope 2 from Carbs = 0.28
Slope 3 from Carbs = 0.15

In order to avoid dealing with two parameters simultaneously, he decides to add another layer of approximation on top of the built-in approximation from the perturbation theory by the following simple averaging formula:

$$\text{Final perturbed PPG} = (A+B)/2$$

Although he decoupled the carbs factor and the walk factor in his perturbation operations, the “measured” PPG dataset and waveform of pre-COVID and COVID periods have actually involved ~19 influential factors with carbs and walk being their 2 primary influential factors.

Results

Figure 1 shows the PPG input data and some calculation results using two perturbation factors for Pre-COVID period (5/5/2018 - 1/18/2020) and COVID period (1/19/2020 - 6/7/2021).

1/19/2020-6/1/21					1/19/2020-6/1/21				
COVID	Carbs	Carbs	Carbs	Pre-COVID	COVID	Walking	Walking	Walking	Pre-COVID
PPG due to Carbs	Measured	Pert A (1st)	Pert A (2nd)	Measured	PPG due to Walking	Measured	Pert A (1st)	Pert A (2nd)	Measured
0 min	120	120	120	120	0 min	120	120	120	120
15 min	122	122	121	120	15 min	122	122	121	121
30 min	125	125	122	121	30 min	125	125	123	121
45 min	128	127	124	122	45 min	128	127	124	122
60 min	126	126	124	122	60 min	126	126	124	122
75 min	123	126	123	122	75 min	123	126	123	122
90 min	120	125	122	121	90 min	120	125	123	121
105 min	118	123	122	121	105 min	118	123	122	121
120 min	116	122	121	120	120 min	116	122	121	121
135 min	115	121	121	120	135 min	115	121	121	120
150 min	116	121	121	120	150 min	116	121	121	120
165 min	117	121	121	120	165 min	117	121	121	120
180 min	118	121	121	120	180 min	118	121	121	120
Average	120.3	123.4	121.7	120.8	Average	120.3	123.4	121.8	120.9
Accuracy (vs. COVID)	97.4%	98.9%	99.4%		Accuracy (vs. COVID)	97.4%	98.7%	99.4%	
Correlation (vs. COVID)	81%	81%	81%		Correlation (vs. COVID)	81%	81%	81%	
Carbs & Walking	High-carbs	Selected	Low-carbs	Conversion %	Carbs & Walking	High-walk	Selected	Low-walk	Conversion %
Selection of Carbs	21.8	13.2	4.9	0.93	Selection of Carbs	25.9	43.6	30.7	0.93
Perturbation Theory	1st order	2nd order	3rd order		Perturbation Theory	1st order	2nd order	3rd order	
(Select-Low/High-Low)	Slope	0.49	0.24	0.12	(Select-Low/High-Low)	Slope	0.52	0.27	0.14

Figure 1: Input data and calculation results using 2 perturbation factors for two periods of Pre-COVID (5/5/2018 - 1/18/2020) and COVID (1/19/2020 - 6/7/2021)

The first perturbation factor is Carbs of which he has chosen the selected carbs of 13.2 grams. This is his actual measured carbs/sugar amount in the COVID period and is located approximately at the midpoint (13.4 grams) of his low-bound carbs of 4.9 grams and high-bound carbs of 21.8 grams. The three calculated slopes are 0.49 for the first-order perturbation, 0.24 for the second-order perturbation, and 0.12 for the third-order perturbation.

The second perturbation factor is Walk. He has chosen the selected walk of 4,356 steps which is his actual measured carbs/sugar amount in COVID period and is located in the midpoint (4,303 steps) of his low-bound walk of 3,076 steps and high-bound walk of 5,529 steps. The three calculated slopes are 0.52 for the first-order perturbation, 0.27 for the second-order perturbation, and 0.14 for the third-order perturbation.

Figure 2 illustrates three Perturbed PPG curves and one measured PPG curve using 2 perturbation factors for both pre-COVID period (5/5/2018 - 1/18/2020) and COVID period (1/19/2020 - 6/7/2021).

(1/19/20-6/1/21)	COVID	Carbs+Walk	Carbs+Walk	Carbs+Walk
PPG due to Carbs	Measured	Pert A (1st)	Pert A (2nd)	Pert A (3rd)
0 min	120	120	120	120
15 min	122	122	121	121
30 min	125	125	123	121
45 min	128	127	124	122
60 min	126	128	124	122
75 min	123	126	123	122
90 min	120	125	123	121
105 min	118	123	122	121
120 min	116	122	121	121
135 min	115	121	121	120
150 min	116	121	121	120
165 min	117	121	121	120
180 min	118	121	121	120
Average	120.3	123.4	121.8	120.9
Accuracy	100%	97.4%	98.8%	99.5%
Correlation	100%	81%	81%	81%

Figure 2: 3 Perturbed PPG curves and 1 measured PPG curve using 2 perturbation factors for both pre-COVID period (5/5/2018 - 1/18/2020) and COVID period (1/19/2020 - 6/7/2021)

Figure 3 reflects a comparison of 3 perturbed PPG waveforms (using 2 perturbation factors and the pre-COVID measured data as their baselines) versus the measured PPG waveform of COVID period (1/19/2020 - 6/7/2021).

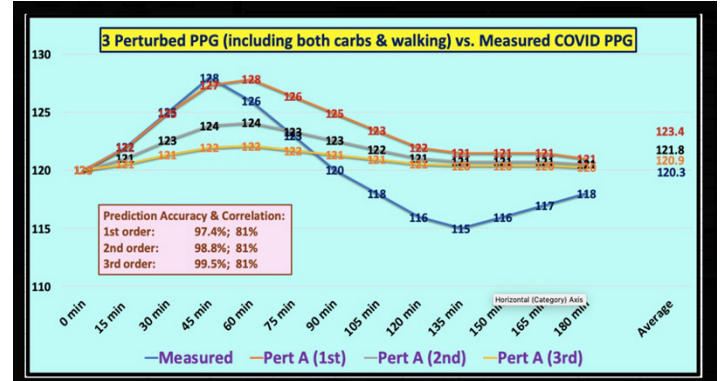


Figure 3: Comparison of 3 perturbed PPG waveforms (using 2 perturbation factors and the pre-COVID measured data as their baselines) versus the measured PPG waveform of COVID period (1/19/2020 - 6/7/2021)

The peak PPG values of the three perturbed curves are 122-128

mg/dL around 60-minutes in comparison with the peak measured COVID curve of 128 mg/dL at 45 minutes. However, these three perturbed PPG waveforms, which are similar to the pre-COVID PPG waveform, are gradually declining after 60-minutes to 180-minutes. On the contrary, the measured COVID PPG waveform has a slight curve tilting-upward after 135-minutes.

The average PPG value and prediction accuracy using two perturbation factors, Carbs and walk, of each perturbation equation for the COVID period are listed below:

Measured: 120.3 mg/dL, 100%
First-order: 123.4 mg/dL, 97.4%
Second-order: 121.8 mg/dL, 98.8%
Third-order: 120.9 mg/dL, 99.5%

The three perturbed waveform predictions have the same shape similarity (i.e., same correlation coefficients of $R=81\%$) in comparison against the measured COVID PPG. These slightly lower than 90% of R is due to the fact that the 3 predicted COVID waveforms are using the pre-COVID measured data as their baseline of calculation. Nevertheless, an 81% correlation is still considered as an extremely high number in terms of waveform shape similarity comparison.

The mathematical power of achieving excellent approximation of PPG values and their corresponding waveforms by using the perturbation theory can be observed clearly via the summarized table shown below in the format of first-order, second-order, third-order:

Correlation: 81%, 81%, 81%
Accuracy: 97.4%, 98.8%, 99.5%

As a comparison, the following table reveals the results from using the same high-order perturbation equation but with only one perturbation factor, carbs/sugar intake amount.

Correlation: 81%, 81%, 81%
Accuracy: 97.3%, 98.7%, 99.4%

The results from using only one perturbation factor, carbs, have 0.1% lower prediction accuracy and the same waveform shape similarity of 81% in comparison with the results from using two perturbation factors, i.e. carbs combined with walk.

Conclusions

In summary, the obvious conclusion drawn from this research work is that *the perturbation equation with two perturbation factors provide a predicted PPG with a slightly higher accuracy and near-duplicative waveform shapes in comparison with one perturbation factor. As a matter of fact, the higher-order of the perturbation equation used, the better results can be achieved for prediction accuracy.*

The following table shows the prediction accuracies in the format of (carbs only and carbs combined with walk):

First order: 97.3%, 97.4%

Second order: 98.7%, 98.8%
Third order: 99.4%, 99.5%

In this study, the three perturbed PPG waveforms have equal level of waveform shape similarity with 81% versus the measured COVID PPG waveform. The correlations of lower than 90% are due to the selection on the pre-COVID PPG data as his baseline of calculation.

In the real world, there are very few diabetes doctors and patients who can understand the perturbation theory of quantum mechanics, let alone be able to apply this theory on calculation of predicted future glucose based on previous data, also including two perturbation factors, with a desired high prediction accuracy [1-38].

References

1. Hsu Gerald C (2021) Biomedical research using GH-Method: math-physical medicine, version 3 (No. 386).
2. Hsu Gerald C (2021) From biochemical medicine to math-physical medicine in controlling type 2 diabetes and its complications (No. 387).
3. Hsu Gerald C (2021) Methodology of medical research: Using big data analytics, optical physics, artificial intelligence, signal processing, wave theory, energy theory and transforming certain key biomarkers from time domain to frequency domain with spatial analysis to investigate organ impact by relative energy associated with various medical conditions (No. 397).
4. Hsu Gerald C (2021) Linear relationship between carbohydrates & sugar intake amount and incremental PPG amount via engineering strength of materials using GH-Method: math-physical medicine, Part 1 No. 346.
5. Hsu Gerald C (2021) Investigation on GH modulus of linear elastic glucose with two diabetes patients data using GH-Method: math-physical medicine, Part 2 No. 349.
6. Hsu Gerald C (2021) Investigation of GH modulus on the linear elastic glucose behavior based on three diabetes patients' data using the GH-Method: math-physical medicine, Part 3 No. 349.
7. Hsu Gerald C (2021) Coefficient of GH.f-modulus in the linear elastic fasting plasma glucose behavior study based on health data of three diabetes patients using the GH-Method: math-physical medicine, Part 4 No. 356. J App Mat Sci & Engg Res 4: 50-55.
8. Hsu Gerald C (2020) High accuracy of predicted postprandial plasma glucose using two coefficients of GH.f-modulus and GH.p-modulus from linear elastic glucose behavior theory based on GH-Method: math-physical medicine, Part 5 No. 357. J App Mat Sci & Engg Res 4: 71-76.
9. Hsu Gerald C (2021) Improvement on the prediction accuracy of postprandial plasma glucose using two biomedical coefficients of GH-modulus from linear elastic glucose theory based on GH-Method: math-physical medicine, Part 6 No. 358.
10. Hsu Gerald C (2021) High glucose predication accuracy of postprandial plasma glucose and fasting plasma glucose during the COVID-19 period using two glucose coefficients of GH-modulus from linear elastic glucose theory based on GH-Method: math-physical medicine, Part 7 No. 359.

11. Hsu Gerald C (2021) Investigation of two glucose coefficients of GH.f-modulus and GH.p-modulus based on data of 3 clinical cases during COVID-19 period using linear elastic glucose theory of GH-Method: math-physical medicine, Part 8 No. 360.
12. Hsu Gerald C (2020) Postprandial plasma glucose lower and upper boundary study using two glucose coefficients of GH-modulus from linear elastic glucose theory based on GH-Method: math-physical medicine, Part 9 No. 361. *J App Mat Sci & Engg Res* 4: 83-87.
13. Hsu Gerald C (2020) Six international clinical cases demonstrating prediction accuracies of postprandial plasma glucoses and suggested methods for improvements using linear elastic glucose theory of GH-Method: math-physical medicine, Part 10 No. 362. *J App Mat Sci & Engg Res* 4: 88-91.
14. Hsu Gerald C (2021) A special Neuro-communication influences on GH.p-modulus of linear elastic glucose theory based on data from 159 liquid egg and 126 solid egg meals using GH-Method: math-physical medicine, Part 11 No. 363. *J App Mat Sci & Engg Res* 5: 126- 131.
15. Hsu Gerald C (2020) GH.p-modulus study of linear elastic glucose theory based on data from 159 liquid egg meals, 126 solid egg meals, and 2,843 total meals using GH-Method: math-physical medicine, Part 12 No. 364. *J App Mat Sci & Engg Res* 4: 31-36.
16. Hsu Gerald C (2020) Detailed GH.p-modulus values at 15-minute time intervals for a synthesized sensor PPG waveform of 159 liquid egg meals, and 126 solid egg meals using linear elastic glucose theory of GH-Method: math-physical medicine, Part 13 No. 365. *J App Mat Sci & Engg Res* 4: 37-42.
17. Hsu Gerald C (2020) A lifestyle medicine model for family medical practices based on 9-years of clinical data including food, weight, glucose, carbs/sugar, and walking using linear elastic glucose theory and GH-Method: math-physical medicine (Part 14) No. 367. *MOJ Gerontol Ger* 5: 197-204.
18. Hsu Gerald C (2020) GH.p-modulus study during 3 periods using finger-piercing glucoses and linear elastic glucose theory (Part 15) of GH-Method: math-physical medicine No. 369. *J App Mat Sci & Engg Res* 4:31-36.
19. Hsu Gerald C (2020) GH.p-modulus study using both finger and sensor glucoses and linear elastic glucose theory (Part 16) of GH-Method: math-physical medicine (No. 370). *J App Mat Sci & Engg Res* 4: 62-64.
20. Hsu Gerald C (2020) A summarized investigation report of GH.p-modulus values using linear elastic glucose theory of GH-Method: math-physical medicine, Part 17 No. 371. *J App Mat Sci & Engg Res* 5: 113-118.
21. Hsu Gerald C (2021) An experimental study on self-repair and recovery of pancreatic beta cells via carbs/sugar intake increase and associated postprandial plasma glucose variation using linear elastic glucose theory (part 18) and GH-Method: math-physical medicine No. 396.
22. Hsu Gerald C (2021) Analyzing roles and contributions of fasting plasma glucose, carbs/sugar intake amount, and post-meal walking steps on the formation of postprandial plasma glucose using Linear Elastic Glucose Theory of GH-Method: math-physical medicine, LEGT Part 19 No. 401.
23. Hsu Gerald C (2021) Analyzing relations among weight, FPG, and PPG using statistical correlation analysis and Linear Elastic Glucose Theory of GH-Method: math-physical medicine, LEGT Part 20 No. 402.
24. Hsu, Gerald C (2021) Estimating cardiovascular disease risk and insulin resistance via transforming glucose wave fluctuations from time domain into associated energy in frequency domain and applying the linear elastic glucose theory of GH-Method: math-physical medicine, LEGT Part 21 No. 403.
25. Hsu Gerald C (2021) PPG magnitude and fluctuation study of three 346-days periods using time-domain and frequency domain analyses as well as linear elastic glucose theory (part 22) of GH-Method: math-physical medicine No. 411.
26. Hsu Gerald C (2021) Using 12-years glucoses including intermittent fasting glucose data, and high-carbs meals glucose data to study the suitability, lower-bound, and upper-bound of the linear elastic glucose theory based on GH-Method: math-physical medicine, Part 23 (No. 412).
27. Hsu Gerald C (2021) A case study of pre-virus period versus virus period applying wave theory, energy theory, Fourier transform, and linear elastic glucose theory (LEGT Part 24) to estimate risk probability of having a cardiovascular disease or stroke and achieving longevity based on GH-Method: math-physical medicine (No. 413).
28. Hsu Gerald C (2021) A case study of three time periods applying wave theory, energy theory, Fourier transform, and linear elastic glucose theory (LEGT Part 25) to estimate risk probability of having a cardiovascular disease or stroke and achieving longevity based on GH-Method: math-physical medicine (No. 414).
29. Hsu Gerald C (2021) A summary report of 25 research articles utilizing linear elastic glucose theory based on GH-Method: math-physical medicine, LEGT Part 26 (No. 415).
30. Hsu Gerald C (2021) An artificial intelligence model applying linear elastic glucose theory to control diabetes and its complications to achieve longevity based on GH-Method: math-physical medicine, LEGT Part 27 (No. 416).
31. Hsu Gerald C (2017) Three GH-modulus for predicted glucose via LEGT linear PPG and HbA1C control based on 12-years lifestyle data and finger-pierced glucoses using GH-Method: math-physical medicine, LEGT Part 28 (No. 417).
32. Hsu Gerald C (2020) Applying first-order perturbation theory of quantum mechanics to predict and build a postprandial plasma glucose waveform (GH-Method: math-physical medicine) No. 152. *Journal of Geriatric Research* 4: 1-2.
33. Hsu Gerald C (2020) Applying the first-order interpolation perturbation method to establish predicted PPG waveforms based on carbs/sugar intake amounts using GH-Method: math-physical medicine (No.154). *J App Mat Sci & Engg Res* 4: 65-70.
34. Hsu Gerald C (2021) Application of perturbation theory, frequency domain energy theory, and linear elasticity theory to study and predict postprandial plasma glucose behaviors and their impact on internal organs of Type 2 diabetes patients based on GH-Method: math-physical medicine (No. 423).
35. Hsu Gerald C (2021) Application of perturbation theory and linear elasticity glucose theory (LEGT Part 31) on postprandial plasma glucose waveform of a single lunch based on

-
- GH-Method: math-physical medicine (No. 424).
36. Hsu Gerald C (2021) Application of higher-order interpolation perturbation theory on postprandial plasma glucose waveform of a single lunch based on GH-Method: math-physical medicine (No. 426).
37. Hsu Gerald C (2021) Application of the first, second, and third order equations of interpolation perturbation theory from quantum mechanics to predict a synthesized 3-year postprandial plasma glucose wave based on GH-Method: math-physical medicine (No. 460).
38. Hsu Gerald C (2021) Predict FPG values of COVID period (using the pre-COVID data as the baseline) applying the higher order equations of interpolation perturbation theory from quantum mechanics and weight as the perturbation factor based on GH-Method: math-physical medicine (No. 463).

Copyright: ©2021 Gerald C Hsu. This is an open-access article distributed under the terms of the Creative Commons Attribution License, which permits unrestricted use, distribution, and reproduction in any medium, provided the original author and source are credited.